ACS APPLIED MATERIALS & INTERFACES

Research Article

Cite This: ACS Appl. Mater. Interfaces 2019, 11, 41668−41675

www.acsami.org

Dynamic Tunable Color Display Based on Metal−Insulator−Metal Resonator with Polymer Brush Insulator Layer as Signal Transducer

Dan Chen,[†,§] Tieqiang Wang,[*,†,‡,§] Guoshuai Song,[†] Yunhao Du,[‡] Jinqiu Lv,[†] Xuemin Zhang,[†] Yunong Li,[†] Liying Zhang,[†] Jianshe Hu,[*,†] Yu Fu,[*,†] and Rainer Jordan[‡]

[†]College of Sciences, Northeastern University, Shenyang 110819, P. R. China

[‡]Chair of Macromolecular Chemistry, School of Science, Technische Universität Dresden, Dresden 01069, Germany

Supporting Information

ABSTRACT: Dynamic color-changing nanomaterials have been widely investigated for applications in fields like optical sensors, wearable activity monitors, smart electronic devices, and anticounterfeiting materials due to the excellent ability to change their optical properties with external variation. Here, a simple metal−insulator−metal (MIM) trilayer Fabry−Perot resonance cavity with a poly(N-isopropylacrylamide) (PNIPAm) brush layer as a responsive element is reported as a thermal-induced colorimetric response platform. The dynamic changes of conformation and physical properties of PNIPAm brush layer in response to external signals give rise to a significant color change of the MIM Fabry−Perot resonance cavity. This MIM Fabry−Perot resonance cavity shows the advantages of dynamic color change, rapid response, good repeatability, and simple construction. Additionally, the as-prepared MIM cavity shows great potential in various applications such as color printing, multicolor indicator, and information anticounterfeiting.

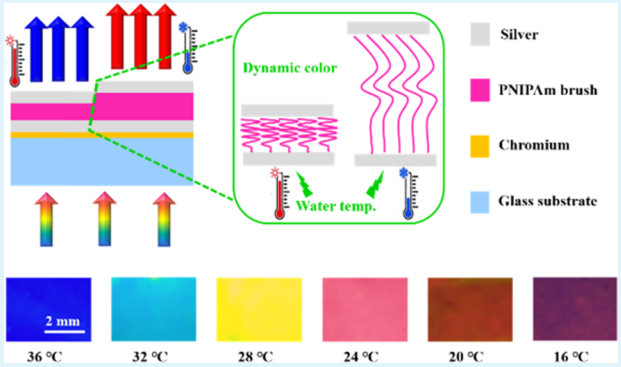

KEYWORDS: *dynamic color, PNIPAm brush, patterns, MIM resonator, nanomaterials*

INTRODUCTION

Structural colors originated from nanostructured materials that interfere with a certain wavelength of light have drawn increasing attention for the advantages of durability, striking brilliance, and high purity.[1−9] To achieve advanced functionalities such as optical sensing, activity monitoring, camouflage and highly secure encryption, scientists have focused on the research of dynamic structural colors.[10,11] It is found that certain animals or insects in nature can produce adaptive colors resulting from special dynamic color-changing nanostructures on their bodies. For instances, chameleons change the lattice spacing of iridophores to adapt to their surroundings; the blue morpho butterfly shows iridescence on the wings due to the swelling of the hierarchical nanostructure in humidity.[12,13] With the inspiration of these special nanostructures, artificial dynamic color-changing nanostructures were developed to mimic complex performance in nature. As the most commonly studied dynamic color-changing nanostructures, photonic crystals show optical responses to external stimulus by introducing stimuli-responsive materials to constitute structures or infiltrate into the interstice of the lattice.[14−16] However, the fabrication of photonic crystals is complicated and time-consuming, which greatly limits the practicalities for real implementation. Plasmonic nanostructures have recently emerged as another type of dynamic color-changing nanostructures with the excellent ability to control optical resonance by adjusting its geometrical parameters and chemical surroundings.[17−19] Especially, utilizing the dynamic response of stimuli-responsive polymer to an external stimulus, many studies have successfully realized the dynamic manipulation of the optical property of plasmonic nanostructures by exploiting stimuli-responsive polymer as responsive components.[20−24] In addition, the miniaturization of plasmonic nanostructures enables the generation of extremely high-resolution color images.[25] So far, unfortunately, only a few methods have been explored to tune the dynamic color of plasmonic nanostructures, which is limited by their structural complexity.[26] Hence, it is highly desired to develop new dynamic color-changing nanomaterials with simple construction and dynamic adjustable color-changing property to meet the requirements of advanced commercial applications.

Fabry−Perot resonance cavities have been commonly investigated for the great potential application in various optical devices. Particularly, by simply controlling the thickness of the insulator layer, metal−insulator−metal (MIM) triple layer based Fabry−Perot resonance cavities are capable of manipulating the incident light in a wide region, which makes them an outstanding candidate in structural coloration.

Received: August 12, 2019
Accepted: October 18, 2019
Published: October 18, 2019

DOI: 10.1021/acsami.9b14125
ACS Appl. Mater. Interfaces 2019, 11, 41668−41675

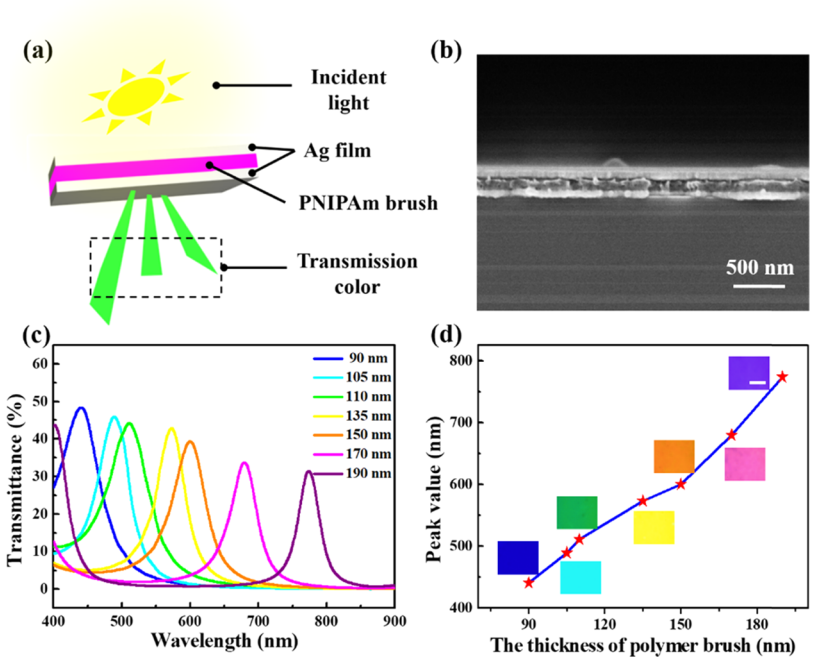

Figure 1. (a) Basic configuration of the MIM Fabry–Perot resonance cavity. (b) Cross-sectional SEM image of the MIM Fabry–Perot resonance cavity. (c) Complete transmission spectra of samples with different thicknesses of PNIPAm brush layer. (d) Plot of the wavelength of the transmission peaks as a function of the PNIPAm layer thickness and corresponding transmission photographs (inset).

Additionally, the manufacturing process is simple, cost-effective, and time-saving.[27] If a kind of stimuli-responsive material is employed as the insulator layer, it is feasible to endow the Fabry–Perot resonance cavity with the dynamic adjustable color-changing property. In previous research, the structural color of a novel Fabry–Perot resonator containing an insulator layer of silk protein changed when it was immersed in water.[28] However, as the swelling of the silk layer is limited by crosslinked networks, the Fabry–Perot resonator shows a slow response rate and the structural color lacks dynamic adjustability. Compared with bulk crosslinked stimuli-responsive polymer, the movement of stimuli-responsive polymer brush chains is more flexible and the conformation change is much easier without limitation of crosslinked networks. More importantly, stimuli-responsive polymer brushes show dramatic changes of conformation and physical property in response to small external stimulus, thus, introducing a stimuli-responsive polymer brush as the insulator layer of the Fabry–Perot resonance cavity may be an alternative approach to achieve dynamic adjustable colors.[29] In addition, stimuli-responsive polymer brushes occupy tremendous advantage in reversible conformational changes and stability, which is beneficial to improve the response performance and repeatability of the resulting Fabry–Perot resonance cavity.[30]

Herein, we report a new dynamic color-changing material based on a Fabry–Perot resonance cavity, which exploits a poly(N-isopropylacrylamide) (PNIPAm) polymer brush insulating layer as a responsive element. The PNIPAm brush layer swells rapidly in response to external temperature variations, which gives rise to a visual transmission color change of the Fabry–Perot resonance cavity in an instant. Benefit from the unique property of the PNIPAm brush layer, the as-prepared Fabry–Perot resonance cavity can be used as an optical temperature indicator with the advantages of rapid response rate and good repeatability. What is more, incorporating the facile microcontact printing technology, various patterns of the Fabry–Perot resonance cavity can be realized in different dimensions. Meanwhile, because the color of the formed patterns is dynamically adjustable with the temperature variations, the as-prepared patterned Fabry–Perot resonance cavity is used in applications such as multicolor indicators and information encryption devices. By exploiting diverse stimuli-responsive polymer brushes, this design strategy would be generally accessible to various functionalities and offers a novel idea for the development of dynamic color-changing materials.

EXPERIMENTAL SECTION

Materials. Glass substrates were immersed in piranha solution (V/V = 3:1 concentrated H_2SO_4/30% H_2O_2) for 4 h at 80 °C to clean and hydroxylate the surface, and then washed several times with deionized water to remove residue reagent. The glass substrate was rinsed with ethanol and dried with a stream of pure nitrogen gas before use. Silver powder (99.9%) and methanol were purchased from Sinopharm Chemical Reagent Co., Ltd. Copper (I) bromide (99%) was obtained from Energy Chemical. N-isopropylacrylamide (NIPAAm) was bought from Tokyo Chemical Industry. Pentamethyldiethylenetriamine and 1-dodecanethiol (98%) were purchased from Aldrich. All chemicals were used as received except CuBr. The CuBr was recrystallized before use. The sulfide initiator, ω-mercaptoundecyl bromoisobutyrate (MUBiB), was synthesized according to a literature procedure.[31]

Preparation. First, a 3 nm thick layer of chromium (Cr) was deposited vertically onto the top of a glass substrate by a thermal evaporator at a rate of 0.5 Å·s^{-1}, which was used as an adhesion layer. Then, a 30 nm thick layer of silver (Ag) was deposited onto the developed samples with a deposition rate of 1 Å·s^{-1}. A layer of PNIPAm brush was polymerized onto the Ag film substrate through a surface-initiated atom transfer radical polymerization (SI-ATRP) technique as reported before.[32] Different thicknesses of polymer brushes could be obtained by changing the concentration of NIPAm. Finally, a 30 nm thick layer of Ag was deposited vertically as a top

DOI: 10.1021/acsami.9b14125
ACS Appl. Mater. Interfaces 2019, 11, 41668–41675

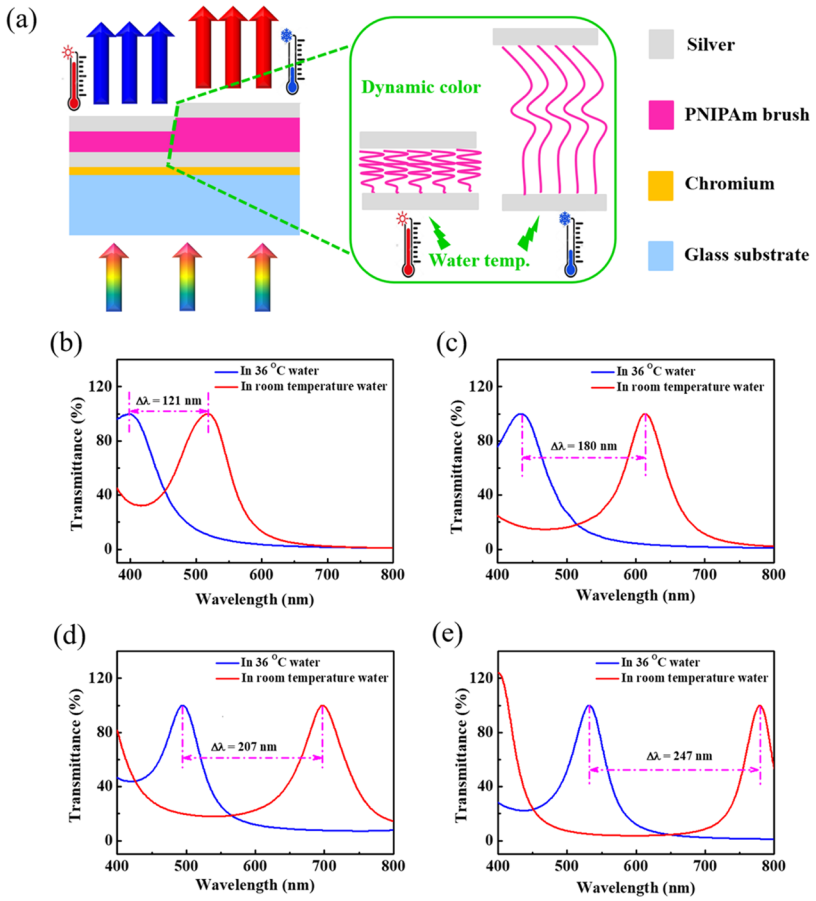

Figure 2. (a) Dynamic color-changing mechanism of the MIM Fabry–Perot resonance cavity. (b–e) Transmission spectra of the as-prepared temperature-responsive MIM Fabry–Perot resonance cavity measured in 36 °C water (blue line) and room temperature water ($T \approx 24$ °C, red line). The thicknesses of the PNIPAm brush middle layer in the MIM Fabry–Perot resonance cavity are (a) 60 nm, (b) 80 nm, (c) 90 nm, and (d) 105 nm, respectively.

layer, forming a MIM Fabry–Perot resonance cavity with the PNIPAm brush layer as the insulator layer.

The multicolor Fabry–Perot resonance cavity was fabricated using a patterned PNIPAm brush layer as the insulator layer. The patterned PNIPAm brush layer was prepared via the combination of a microcontact printing technique and an SI-ATRP process. First, a patterned poly(dimethylsiloxane) (PDMS) stamp was fabricated as reported before.[31] The PDMS stamp was utilized to print patterned MUBiB SAMs on the Ag film substrate, and then the stamped Ag film substrate was placed into a 3:1 mixture of MUBiB and alkanethiols (v/v) in ethanol to form a lower grafting density of MUBiB on the nonpatterned region. Finally, the ATRP initiators with different grafting density were grafted onto the image area and background area of the Ag film substrate and patterned PNIPAm brush layer with different thicknesses can be realized on the Ag substrate following the ATRP process as above.[33]

Characterization. Scanning electron microscopy (SEM) images were characterized by field emission scanning electron microscopy (Hitachi SU8010). Before imaging, samples were sputter-coated with a 10 nm Pt layer. Atomic force microscopy (AFM) images were recorded using the scanasyst in the air mode and liquid phase mode (AFM, Bruker Dimension Icon). The transmission spectra from 400 to 800 nm were measured with an optics spectrometer (Ocean Optics, Maya 2000PRO). The responsive performance was evaluated by measuring the transmission spectra of samples in deionized water with different temperatures. A metal heating stage was placed under the sample to control the temperature of the whole system. When the response rate of a sample was measured, the integral time of the Maya spectrometer was set to be 8 ms and the spectra recorded during the measurement were saved automatically in turn. The optical photographs were taken by a fluorescence microscope (Olympus, BX53M).

RESULTS AND DISCUSSION

The MIM Fabry–Perot resonance cavity was prepared through SI-ATRP and thermal evaporation. As illustrated in Figure 1a, the basic configuration of the MIM Fabry–Perot resonance cavity consists of a top silver layer, a middle PNIPAm brush layer, and a bottom silver layer. The cross-sectional SEM image of the as-prepared MIM Fabry–Perot resonance cavity is shown in Figure 1b, which depicts a clear three-layered stacked structure with an insulator layer of subwavelength thickness. A series of samples with different thicknesses of the middle PNIPAm brush layer were fabricated to investigate the color-tunable capability of the MIM Fabry–Perot resonance cavity. As shown in Figure 1c, a transmission spectrum covering the entire visible region is realized by tuning the thickness of PNIPAm brush layer. The thickness of PNIPAm brush layer can be controlled by varying the polymerization condition (Figure S1). Different thicknesses of PNIPAm brush layer were characterized by AFM (Figure S2). Figure 1d shows the plot of the wavelength of the transmission peaks as a function of the PNIPAm layer thickness and corresponding transmission photographs (inset). With the gradual increase of the PNIPAm brush layer from 90 to 190 nm, the first-order transmission peak redshifts, which leads to a vivid, full-color gamut. The linear fitting calculation was performed to analyze the

DOI: 10.1021/acsami.9b14125
ACS Appl. Mater. Interfaces 2019, 11, 41668–41675

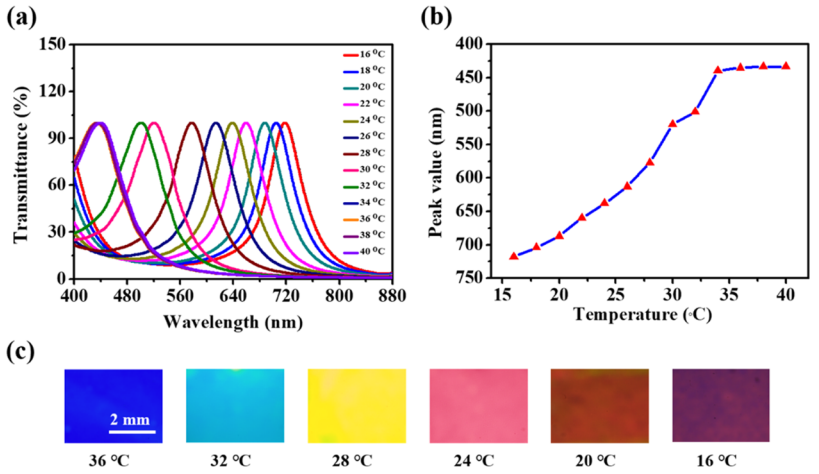

Figure 3. Dynamic color-changing behavior of the MIM Fabry–Perot resonance cavity with an 80 nm PNIPAm brush layer at different temperatures. (a) Transmission spectra of the MIM Fabry–Perot resonance cavity in different temperature of water. (b) Plot of the wavelength of the transmission peaks as a function of the temperature of water. (c) Corresponding dynamic photographs taken by an optical microscope.

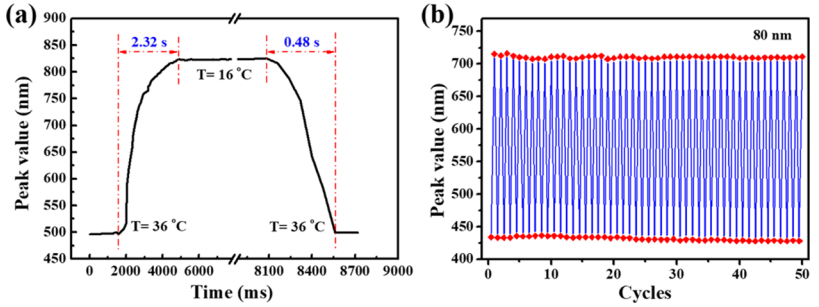

Figure 4. (a) Real-time monitoring of the temperature with the dynamic color-changing material manifested by the transmission peak shift in water temperature change from 36 to 16 °C. (b) Reproducibility of the dynamic color-changing material between hot water (36 °C) and cold water (16 °C).

relationship between the wavelength of transmitted light and the thickness of PNIPAm brush layer, the transmission wavelength λ can be approximated as $\lambda = 154.965 + 3.139d$, where d is the thickness of PNIPAm brush layer.

The dynamic color-changing mechanism of the MIM Fabry–Perot resonance cavity is illustrated in Figure 2a. The PNIPAm brush insulating layer is a thermoresponsive polymer, which undergoes a conformational change and a drastic volume variation at different temperatures.[25] From the results mentioned above, the resonant wavelength of the MIM Fabry–Perot resonance cavity can be influenced by the thickness of the middle PNIPAm brush layer. Therefore, by changing the system temperature, dynamic colors can be produced with the as-prepared MIM Fabry–Perot resonance cavity. To clarify that the top dense Ag layer does not affect the swelling property of the middle PNIPAm brush layer, the total thicknesses of the trilayer structure in air and in room temperature water were characterized by AFM (Figure S3). The swelling ratio of the PNIPAM calculated by the ratio between the thicknesses of the swollen film and original dry film was 2.56. Such a drastic change in the thickness of the middle PNIPAm brush layer endows the MIM Fabry–Perot resonance cavity with a wide tunable color range.

On further investigation, we explored how the responsive optical property of the MIM Fabry–Perot resonance cavity depends on the thickness of PNIPAm brush layer. As shown in Figure 2b–e, the transmission spectra of Fabry–Perot resonance cavities with different thicknesses of PNIPAm brush layer were measured in 36 °C and room temperature water. The sample with a thicker original PNIPAm brush layer showed a greater peak shift ($\Delta\lambda$) (121 nm for the 60 nm sample, 180 nm for the 80 nm sample, 207 nm for the 90 nm sample, and 247 nm for the 105 nm sample), because the swollen thickness of the PNIPAm brush is affected by the original thickness of the PNIPAm brush layer (Figure S4). To achieve dynamic colors covering the whole visible region, it is desirable to select an optimized thickness of PNIPAm brush layer to make the transmission peak shift from the blue region to the red region. Among all of these samples, only the 80 nm sample is capable to realize the color tunability in a full visible region, thus, most of the following discussions are based on the 80 nm sample.

To realize the precise control of the structural color, the transmission spectra and color changes of the MIM Fabry–Perot resonance cavity were further explored in different temperature of water. As shown in Figure 3a, it is clear that the transmission spectra of the MIM Fabry–Perot resonance cavity respond dramatically to different temperature of water. With the increase in water temperature from 16 to 40 °C, the transmission peak shows a strong blue shift from 718 to 440 nm. The plot of the wavelength of the transmission peaks against the temperature of water shown in Figure 3b demonstrates that the peak value becomes stable at around 34 °C. This can be explained by literature reported before, which reveals that the PNIPAm brush layer shrinks in water with higher temperature and collapse while the temperature is

DOI: 10.1021/acsami.9b14125
ACS Appl. Mater. Interfaces 2019, 11, 41668–41675

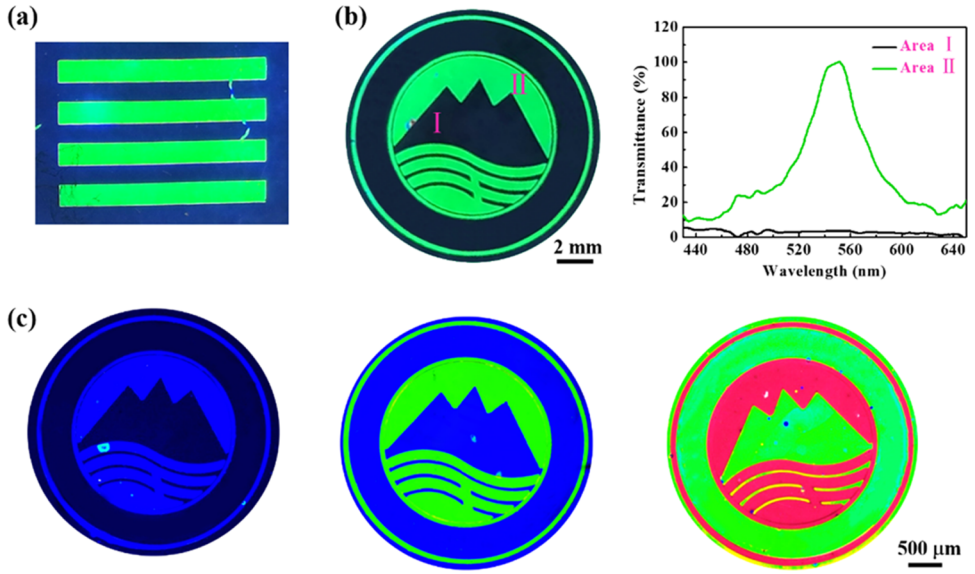

Figure 5. Color patterning of the MIM Fabry–Perot resonance cavity. (a) Stripes pattern, (b, c) school badges of Northeastern University with three primary colors of red, green, and blue, respectively.

above its lower solution critical temperature of ~32 °C.[34] As presented in Figure 3c, the color of the MIM Fabry–Perot resonance cavity experiences a significant change corresponding to the transmission peak shift. Apparently, it exhibits six distinguishable colors of blue, bluish green, yellow, cyan, red, and purplish red for T = 36, 32, 28, 24, 20, and 16 °C, respectively. The dynamic color-changing behavior can be triggered by changing the environmental temperature (Movie S1, Supporting Information).

For optical sensing applications, the response rate is a crucial parameter to evaluate the responsive performance of dynamic color-changing material. Real-time monitoring of transmission peaks was carried out to investigate the response and recovery of the MIM Fabry–Perot resonance cavity between the fully collapsed state and swollen state of the middle PNIPAm brush layer. To obtain better accuracy, the MIM Fabry–Perot resonance cavity was combined with a PDMS microfluidic channel. The PDMS microfluidic channel has a rectangular chamber that was connected to an outlet and an inlet. The surface of the MIM Fabry–Perot resonance cavity was adhered to and exposed to the PDMS microfluidic channel. The inlet and outlet were connected with poly(vinyl chloride) tubing for water transportation. As demonstrated in Figure 4a, when the microfluidic channel is filled with hot water (36 °C), the transmission peak locates at 500 nm. The transmission peak shifts towards the longer wavelength, and reaches a balanced and steady-state after 2.32 s while replacing the hot water (36 °C) with cold water (16 °C). In the reverse direction, from cold water (16 °C) to hot water (36 °C), the recovery time is 0.48 s, which is much faster than response time. It is still worthy to note that the response rate of the MIM Fabry–Perot resonance cavity, compared with other stimuli-responsive materials based on bulk polymers reported previously, was dramatically enhanced by introducing a polymer brush layer as a responsive part, because the movement of polymer brush chains is more flexible and the conformation change is much easier without limitation of crosslinked networks.[30]

Except for the response rate, the reproducibility is another important parameter to evaluate the reliability of dynamic color-changing material. The reproducibility of the as-prepared dynamic color-changing material was performed in water under 16 and 36 °C (Figure S5). As shown in Figure 4b, after 50 cycles, the position of transmission peak shows nearly no change, which demonstrates that the dynamic color-changing material still remains highly stable. In addition, after the repeatability test, the sample is still able to respond to external temperature change in 3 months when it is kept in nitrogen atmosphere. The dynamic color-changing material exhibits high repeatability due to covalent bonding of PNIPAm brush molecules with the Ag film substrate, which makes the responsive structure more stable.

As an optical material, it is meaningful to conduct the miniaturization and integration of the Fabry–Perot resonance cavity. It is noteworthy that the structural color can be tuned by varying the thickness of the middle PNIPAm brushes layer. On the other hand, through the SI-ATRP process, different thicknesses of polymer brush can be obtained by varying the grafting density of initiators.[35] In this work, based on the facile microcontact printing technology, patterned PNIPAm brushes with a thickness difference in the image area and background area were prepared. By introducing a patterned PNIPAm brush layer as the insulator layer of the Fabry–Perot resonance cavity, different multicolor patterns, such as a stripe pattern and a school badge can be achieved as shown in Figure 5a,b. The image area of the school badge was green, corresponding to a transmission peak at 550 nm, while the black background area shows no resonant peak in the visible region due to an ultrathin PNIPAm brush layer. Then, using a PDMS stamp with microdimension, micropatterned school badges with three primary colors of red, green, and blue shown in Figure 5c could also be obtained by simply tuning the thickness of PNIPAm brush layer. As shown in Figure S6, to clarify the resolution of this MIM Fabry–Perot resonance cavity, the micropatterns with a smaller size were fabricated. These examples demonstrate that this proposed MIM Fabry–Perot resonance cavity shows great potential in the color printing.

The color-changing behavior of the patterned MIM Fabry–Perot resonance cavity was further investigated. As shown in Figure 6a, when the as-prepared school badge was immersed in hot water, the image area was orange in color and the

DOI: 10.1021/acsami.9b14125
ACS Appl. Mater. Interfaces 2019, 11, 41668–41675

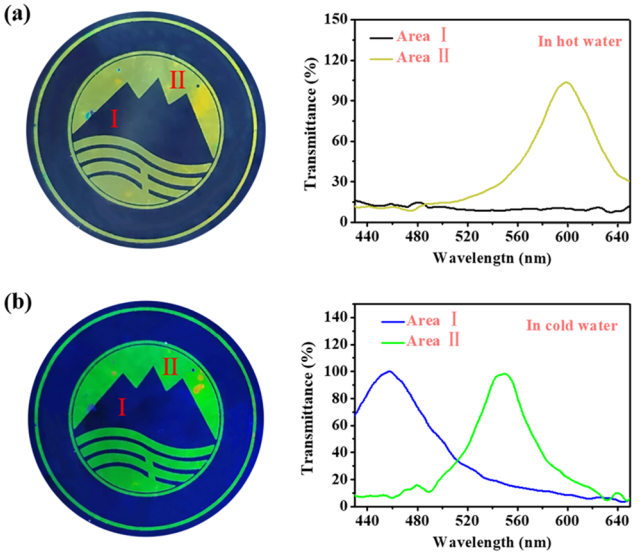

Figure 6. Temperature-induced color-changing behavior of the patterned MIM Fabry–Perot resonance cavity. Normalized transmission spectra and the corresponding photographs in (a) room temperature water ($T \approx 18$ °C) and (b) hot water ($T > 40$ °C).

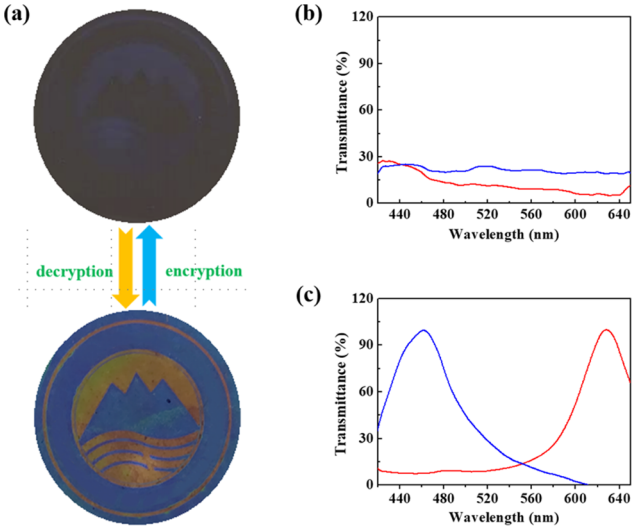

Figure 7. Information encryption device based on the temperature-induced color-changing property. The encrypted and decrypted badges (a) and their corresponding normalized transmission spectra in air (b) and in room temperature water (c).

background area was black. The resonance peak of the background area did not appear in the visible region due to an ultrathin PNIPAm brush layer, resulting in the generation of black color. When the hot water was replaced by room temperature water, both the color in the image area and background area changed significantly due to the dramatic swelling of the PNIPAm brush layer (Figure 6b). The color of the image area changed from yellow to green, because the first-order transmission peak redshifts to the infrared region and the second-order transmission peak redshifts into the visible region. This patterned MIM Fabry–Perot resonance cavity shows temperature-induced color-changing capability and features great potentials in dynamic multicolor printing.

Except for the application of dynamic multicolor printing, the patterned MIM Fabry–Perot resonance cavity can also serve as an information encryption device. When the thicknesses of the PNIPAm on the image and background area are both thin enough, the encoded pattern is difficult to be observed in air. After being exposed to the cold water, the encrypted information appeared because of the drastic swelling of PNIPAm brush layer. As presented in Figure 7a, the encrypted badge pattern emerges instantly when the MIM Fabry–Perot resonance cavity is immersed in the cold water. The corresponding transmission spectra of the encrypted pattern and the decrypted pattern are presented in Figure 7b,c. After the sample is dried by N_2, the badge pattern was hidden again. The encrypted information can be hidden well in air condition unless exposed to cold water.

CONCLUSIONS

In summary, a novel dynamic color-changing material based on an MIM Fabry–Perot resonance cavity with a responsive PNIPAm brush layer as the insulating layer was reported. This simple construction does not require any elaborate manufacturing method compared with other dynamic color-changing materials such as photonic crystals and plasmonic nanostructures. Moreover, the MIM Fabry–Perot resonance cavity responds to external temperature variations quickly, which appears as a dramatic change of spectrum signal. Thus, the structural color could be dynamically adjustable by varying the external temperature. The reversible conformational changes and stability of PNIPAm brush endow the MIM Fabry–Perot resonance cavity with a rapid response rate and good reproducibility. Meanwhile, owing to the facile microcontact printing technology, various patterns of the Fabry–Perot resonance cavity can be realized in different dimensions, and the dynamic color-changing capability facilitates the applications of multicolor indicators and information encryption devices. Since stimuli-responsive polymer brushes are diverse, this design strategy would be general for achieving diverse functionalities and offers a novel idea for the development of dynamic color-changing materials. This Fabry–Perot resonance cavity will provide new opportunities in application fields such as optical sensors, display devices, and activity monitors.

ASSOCIATED CONTENT

Supporting Information

The Supporting Information is available free of charge on the ACS Publications website at DOI: 10.1021/acsami.9b14125.

Thickness of PNIPAm; AFM image; measured transmission spectra of the first two cycles and the last two cycles in the repeatability test; color patterning (PDF). Movie about the dynamic color-changing behavior of the patterned Fabry–Perot resonance cavity (Movie S1) (MP4)

AUTHOR INFORMATION

Corresponding Authors

*E-mail: wangtieqiang@mail.neu.edu.cn (T.W.).
*E-mail: hujianshe@mail.neu.edu.cn (J.H.).
*E-mail: fuyu@mail.neu.edu.cn (Y.F.).

ORCID

Tieqiang Wang: 0000-0003-3104-8421
Yunong Li: 0000-0002-0872-5976
Yu Fu: 0000-0003-0962-7152

DOI: 10.1021/acsami.9b14125
ACS Appl. Mater. Interfaces 2019, 11, 41668–41675

Author Contributions

[§]D.C. and T.W. contributed equally.

Notes

The authors declare no competing financial interest.

■ ACKNOWLEDGMENTS

This work was supported by the National Natural Science Foundation of China (21805028 and 21805029), Fundamental Research Funds for the Central Universities (N160504002, N170503010, N180504005, N180705004, N180402023, and N180504007), and Open Project of State Key Laboratory of Supramolecular Structure and Materials (sklssm201906, sklssm2019027, and sklssm2019038).

■ REFERENCES

(1) Zhao, Y.; Xie, Z.; Gu, H.; Zhu, C.; Gu, Z. Bio-inspired Variable Structural Color Materials. *Chem. Soc. Rev.* **2012**, *41*, 3297−3317.

(2) Xiao, M.; Hu, Z.; Wang, Z.; Li, Y.; Tormo, A. D.; Le Thomas, N.; Wang, B.; Gianneschi, N. C.; Shawkey, M. D.; Dhinojwala, A. Bioinspired Bright Noniridescent Photonic Melanin Supraballs. *Sci. Adv.* **2017**, *3*, No. e1701151.

(3) Kristensen, A.; Yang, J. K. W.; Bozhevolnyi, S. I.; Link, S.; Nordlander, P.; Halas, N. J.; Mortensen, N. A. Plasmonic Colour Generation. *Nat. Rev. Mater.* **2017**, *2*, No. 16088.

(4) Fu, F.; Chen, Z.; Zhao, Z.; Wang, H.; Shang, L.; Gu, Z.; Zhao, Y. Bio-inspired Self-healing Structural Color Hydrogel. *Proc. Natl. Acad. Sci. U.S.A.* **2017**, *114*, 5900−5905.

(5) Vignolini, S.; Rudall, P. J.; Rowland, A. V.; Reed, A.; Moyroud, E.; Faden, R. B.; Baumberg, J. J.; Glover, B. J.; Steiner, U. Pointillist Structural Color in Pollia Fruit. *Proc. Natl. Acad. Sci. U.S.A.* **2012**, *109*, 15712−15715.

(6) Kumar, K.; Duan, H.; Hegde, R. S.; Koh, S. C. W.; Wei, J. N.; Yang, J. K. W. Printing Colour at the Optical Diffraction Limit. *Nat. Nanotechnol.* **2012**, *7*, 557−561.

(7) Pi, J.-K.; Yang, J.; Zhong, Q.; Wu, M.-B.; Yang, H.-C.; Schwartzkopf, M.; Roth, S. V.; Müller-Buschbaum, P.; Xu, Z.-K. Dual-Layer Nanofilms via Mussel-Inspiration and Silication for Non-Iridescent Structural Color Spectrum in Flexible Displays. *ACS Appl. Nano Mater.* **2019**, *2*, 4556−4566.

(8) Gensch, M.; Schwartzko, M.; Ohm, W.; Brett, C. J.; Pandit, P.; Vayalil, S. K.; Biessmann, L.; Kreuzer, L. P.; Drewes, J.; Polonskyi, O.; Strunskus, T.; Faupel, F.; Stierle, A.; Muller-Buschbaum, P.; Roth, S. V. Correlating Nanostructure, Optical and Electronic Properties of Nanogranular Silver Layers during Polymer-Template-Assisted Sputter Deposition. *ACS Appl. Mater. Interfaces* **2019**, *11*, 29416−29426.

(9) Schwartzkopf, M.; Santoro, G.; Brett, C. J.; Rothkirch, A.; Polonskyi, O.; Hinz, A.; Metwalli, E.; Yao, Y.; Strunskus, T.; Faupel, F.; Muller-Buschbaum, P.; Roth, S. V. Real-Time Monitoring of Morphology and Optical Properties during Sputter Deposition for Tailoring Metal-Polymer Interfaces. *ACS Appl. Mater. Interfaces* **2015**, *7*, 13547−13556.

(10) Fu, F.; Shang, L.; Chen, Z.; Yu, Y.; Zhao, Y. Bioinspired Living Structural Color Hydrogels. *Sci. Robot.* **2018**, *3*, No. eaar8580.

(11) Aguirre, C. I.; Reguera, E.; Stein, A. Tunable Colors in Opals and Inverse Opal Photonic Crystals. *Adv. Funct. Mater.* **2010**, *20*, 2565−2578.

(12) Potyrailo, R. A.; Ghiradella, H.; Vertiatchikh, A.; Dovidenko, K.; Cournoyer, J. R.; Olson, E. Morpho Butterfly Wing Scales Demonstrate Highly Selective Vapour Response. *Nat. Photonics* **2007**, *1*, 123−128.

(13) Teyssier, J.; Saenko, S. V.; van der Marel, D.; Milinkovitch, M. C. Photonic Crystals Cause Active Colour Change in Chameleons. *Nat. Commun.* **2015**, *6*, No. 6368.

(14) Cai, Z.; Kwak, D. H.; Punihaole, D.; Hong, Z.; Velankar, S. S.; Liu, X.; Asher, S. A. A Photonic Crystal Protein Hydrogel Sensor for *Candida albicans*. *Angew. Chem.* **2015**, *54*, 13228−13232.

(15) Szendrei-Temesi, K.; Sanchez-Sobrado, O.; Betzler, S. B.; Durner, K. M.; Holzmann, T.; Lotsch, B. V. Lithium Tin Sulfide-a High-Refractive-Index 2D Material for Humidity-Responsive Photonic Crystals. *Adv. Funct. Mater.* **2018**, *28*, No. 1705740.

(16) Lee, H.; Jeon, T. Y.; Lee, S. Y.; Lee, S. Y.; Kim, S.-H. Designing Multicolor Micropatterns of Inverse Opals with Photonic Bandgap and Surface Plasmon Resonance. *Adv. Funct. Mater.* **2018**, *28*, No. 1706664.

(17) Zhu, X.; Yan, W.; Levy, U.; Mortensen, N. A.; Kristensen, A. Resonant Laser Printing of Structural Colors on High-index Dielectric Metasurfaces. *Sci. Adv.* **2017**, *3*, No. e1602487.

(18) Zhu, X.; Vannahme, C.; Hojlund-Nielsen, E.; Mortensen, N. A.; Kristensen, A. Plasmonic Colour Laser Printing. *Nat. Nanotechnol.* **2016**, *11*, 325−330.

(19) Duan, X.; Liu, N. Scanning Plasmonic Color Display. *ACS Nano* **2018**, *12*, 8817−8823.

(20) Franklin, D.; Frank, R.; Wu, S.-T.; Chanda, D. Actively Addressed Single Pixel Full-Colour Plasmonic Display. *Nat. Commun.* **2017**, *8*, No. 15209.

(21) Yan, Y.; Liu, L.; Cai, Z.; Xu, J.; Xu, Z.; Zhang, D.; Hu, X. Plasmonic Nanoparticles Tuned Thermal Sensitive Photonic Polymer for Biomimetic Chameleon. *Sci. Rep.* **2016**, *6*, No. 31328.

(22) Cormier, S.; Ding, T.; Turek, V.; Baumberg, J. J. Dynamic- and Light-Switchable Self-Assembled Plasmonic Metafilms. *Adv. Opt. Mater.* **2018**, *6*, No. 1800208.

(23) Ding, T.; Ruettiger, C.; Zheng, X.; Benz, F.; Ohadi, H.; Vandenbosch, G. A. E.; Moshchalkov, V. V.; Gallei, M.; Baumberg, J. J. Fast Dynamic Color Switching in Temperature-Responsive Plasmonic Films. *Adv. Opt. Mater.* **2016**, *4*, 877−882.

(24) Xiong, K.; Emilsson, G.; Maziz, A.; Yang, X.; Shao, L.; Jager, E. W. H.; Dahlin, A. B. Plasmonic Metasurfaces with Conjugated Polymers for Flexible Electronic Paper in Color. *Adv. Mater.* **2016**, *28*, 9956−9960.

(25) Xiong, K.; Tordera, D.; Emilsson, G.; Olsson, O.; Linderhed, U.; Jonsson, M. P.; Dahlin, A. B. Switchable Plasmonic Metasurfaces with High Chromaticity Containing Only Abundant Metals. *Nano Lett.* **2017**, *17*, 7033−7039.

(26) Wang, G.; Chen, X.; Liu, S.; Wong, C.; Chu, S. Mechanical Chameleon through Dynamic Real Time-Plasmonic Tuning. *ACS Nano* **2016**, *10*, 1788−1794.

(27) Li, Z.; Butun, S.; Aydin, K. Large-Area, Lithography-Free Super Absorbers and Color Filters at Visible Frequencies Using Ultrathin Metallic Films. *ACS Photonics* **2015**, *2*, 183−188.

(28) Kwon, H.; Kim, S. Chemically Tunable, Biocompatible, and Cost-Effective Metal-Insulator-Metal Resonators Using Silk Protein and Ultrathin Silver Films. *ACS Photonics* **2015**, *2*, 1675−1680.

(29) Barbey, Rl.; Lavanant, L.; Paripovic, D.; Schüwer, N.; Sugnaux, C.; Tugulu, S.; Klok, H.-A. Polymer Brushes via Surface-Initiated Controlled Radical Polymerization: Synthesis, Characterization, Properties, and Applications. *Chem. Rev.* **2009**, *109*, 5437−5527.

(30) Wang, T.; Yu, Y.; Chen, D.; Wang, S.; Zhang, X.; Li, Y.; Zhang, J.; Fu, Y. Naked Eye Plasmonic Indicator with Multi-responsive Polymer Brush as Signal Transducer and Amplifier. *Nanoscale* **2017**, *9*, 1925−1933.

(31) Shah, R. R.; Merreceyes, D.; Husemann, M.; Rees, I.; Abbott, N. L.; Hawker, C. J.; Hedrick, J. L. Using Atom Transfer Radical Polymerization To Amplify Monolayers of Initiators Patterned by Microcontact Printing into Polymer Brushes for Pattern Transfer. *Macromolecules* **2000**, *33*, 597−605.

(32) Kim, D. J.; Kang, S. M.; Kong, B.; Kim, W.-J.; Paik, H.-j.; Choi, H.; Choi, I. S. Formation of Thermoresponsive Gold Nanoparticle/PNIPAAm Hybrids by Surface-Initiated, Atom Transfer Radical Polymerization in Aqueous Media. *Macromol. Chem. Phys.* **2005**, *206*, 1941−1946.

(33) Cai, S.; Suo, Z. Mechanics and Chemical Thermodynamics of Phase Transition in Temperature-sensitive Hydrogels. *J. Mech. Phys. Solids* **2011**, *59*, 2259−2278.

(34) Wang, X.; Bohn, P. W. Spatiotemporally Controlled Formation of Two-component Counterpropagating Lateral Graft Density

DOI: 10.1021/acsami.9b14125
ACS Appl. Mater. Interfaces 2019, 11, 41668−41675

Gradients of Mixed Polymer Brushes on Planar an Surfaces. *Adv. Mater.* **2007**, *19*, 515−520.
(35) Chen, T.; Jordan, R.; Zauscher, S. Dynamic Microcontact Printing for Patterning Polymer-Brush Microstructures. *Small* **2011**, *7*, 2148−2152.

DOI: 10.1021/acsami.9b14125
ACS Appl. Mater. Interfaces 2019, 11, 41668−41675